IIETA International Information and Engineering Technology Association
Advancing the World of Information and Engineering

Mathematical Modelling of Engineering Problems
Vol. 9, No. 6, December, 2022, pp. 1523-1531
Journal homepage: http://iieta.org/journals/mmep

Sensorless Speed Control of a Brushless DC Motor Using Particle Filter (PF)

Ghufran W. Abedulabbas*, Farazdaq R. Yaseen

Control and Systems Engineering Dept., Univ. of Technology-Iraq, Baghdad 10066, Iraq

Corresponding Author Email: cse.20.05@grad.uotechnology.edu.iq

https://doi.org/10.18280/mmep.090612

Received: 12 September 2022
Accepted: 17 November 2022

Keywords:
brushless direct current (BLDC) motor, Particle Filter (PF), Extended Kalman Filter (EKF)

ABSTRACT

The equivalent of electricity has recently been used to replace all the wear-prone moving mechanical components that produce faults. The electronic unit that substitutes the mechanical commutation unit in Brushless Direct Current (BLDC) motors improves dynamic properties, noise level, and efficiency. This work describes a method for estimating the BLDC machine's rotor speed and position by using Extended Kalman Filter (EKF) and Particle Filter (PF). The BLDC is a non-linear system with nonlinear measurements. To perform the EKF, Jacobian linearization of the motor model and the observation are needed. Linearization leads to a decrease in the accuracy of filter estimation. In PF, the relative likelihood of each particle is computed according to the measurements. Resampling gives set particles are distributed according to power density function (pdf). Then the PF can compute any desired statistical measure of this pdf. A sensorless drive has an accurate good throughout a wide speed range and with varied load torque, according to the simulation's results. The results show that the velocity inaccuracy rate at PF is approximately 0.01% and that at EKF it is approximately 1%. According to the findings, the PF outperformed the EKF in a comparison between them.

1. INTRODUCTION

An improved variant of the standard DC motor is the brushless DC (BLDC) motor, which replaces the commutator and brushes with an electronic commutation mechanism. BLDC motors are utilized in a variety of settings, including industry, the home, computers, automobiles, etc. They are quickly gaining prominence. The 3-phase permanent-magnet synchronous motor is comparable to the 3-phase BLDC motor in terms of construction, while the DC motor is similar in terms of functioning [1]. A 3-phase inverter that functions by the timing indications from the Hall-effect sensor provide the electrical power for the BLDC motor [2, 3]. Sensorless BLDC motors are widely utilized in a variety of applications, including instrumentation, automated industrial machinery, consumer goods, vehicles, and more. Those motors had been utilized in a broad range of the industrial applications due to the fact that their architecture is perfect for any safety-critical application. Sensorless BLDC motors are frequently utilized because of their increased efficiency, dependability, power, and low acoustic noise [4, 5]. A larger speed range, better speed-to-torque characteristics, greater dynamic responsiveness, lower weight, and a longer lifespan the elimination of the motor's neutral voltage, the use of a predetermined phase shift circuit, and its affordability are only a few of its benefits [6, 7]. However, the main disadvantages are the higher cost, the size of the motor, and the requirement for a unique mounting solution for the Sensors [8].

A brushless motor with electronic control is a BLDC. The BLDC needs the sensor position's reading of the rotor position to turn the rotor. It also affects the sensor's high price and dependability, which are problems. Because BLDCM is a brushless motor Then BLDC requires the position of the sensor to rotate the rotor and this is a weakness of BLDC so use other methods such as the Extended Kalman Filter (EKF) to cover this weakness. In addition, BLDC is also a non-linear system. For improving the performance of BLDC motor drives, numerous sensorless control techniques have been presented [9]. Many researchers have developed a sensorless strategy to overcome this problem. The use of BLDC in all industries will be fueled by effective solutions because it is a low-cost and high-reliability solution. In recent decades, numerous sensorless driving methods, like trapezoidal back-EMFs, have been created to take the role of sensor position [10]. There are a lot of researchers who have used algorithms to improve the performance of Brushless DC Motor, in 2021, Ellahi [11] the Extended Kalman filter has been utilized for the estimation of position and speed in this thesis. The DC voltage will be applied first as a source of information The Extended Kalman Filter is employed to perform the analysis. Whereas a PID controller has been used so as to estimate the state following reference signal, and adjust system state. Then, Vinida and Chacko [12] proposed the H_∞ algorithm to enhance the performance of a sensorless BLDC motor whose algorithm weights are optimized by PSO. The proposed controller decreases the percentage overshoot and reduce the settling time. In 2018, Chojowski [13] proposed the EKF to estimates the parameters of the BLDC motor. A critical step in the filter design is the choice of the initial values for the covariance matrices of the plant model (Q) and observation model (R) as they affect the performance, convergence, and stability. Any increase in the values of the Q matrix elements will cause an increase in the Kalman gain. Increasing the values of the elements inside the R matrix will cause a decrease in the

Kalman gain, and this in turn will make the transient response worse.

In, Rif'an et al. [14] presents a new algorithm for a BLDC motor based on the Ensemble Kalman Filter (EnKF) and NN. The EnKF is used to estimate the speed and position of the rotor. The NN is used to estimates the perturbations. The speed error was about 3% with 2 electrical angles during the perturbations of 50%.

In 2015, Lv et al. [15] presented in this paper, a new mathematical model is built according to the characteristics of the brushless DC (BLDC)motor and a new filtering algorithm is proposed for the sensorless BLDC motor based on the unscented Kalman filter (UKF).

The proposed UKF algorithm is employed to estimate the speed and rotor position of the BLDC motor only using the measurements of terminal voltages and three-phase currents. In order to observe the drive performance, two simulation examples are given and the feasibility and effectiveness of the UKF algorithm are verified through the simulation results.

Rif'an et al. [16] methods for BLDC estimation and control are discussed in the abstract. A flaw in BLDC is that it depends on the sensor position to rotate the rotor because BLDCM is a brushless motor. To address this flaw, a sensorless Extended Kalman Filter (EKF) technique was suggested. And BLDC is a non-linear system as well. As a result, using a traditional PID technique makes it impossible to produce an accurate and worthwhile PID parameter controller. A single neural network called a fuzzy PID for BLDC was constructed in this paper. The experimental findings demonstrate that the EKF can estimate the speed of BLDC and single neural networks, and that BLDC system speed is increased by fuzzy PID controller.

In this paper, two modern algorithms are used, namely EKF and PF to measure the velocity of brushless dc motor and position by relying on measuring currents and voltages. through our results. It was noted that this work gave the best result regarding stability at 1s, speed error at 0.01%, and position error at 0.112% compared to previous studies. It is considered the best improvement in system performance.

2. BLDC MOTOR'S MATHEMATICAL MODEL

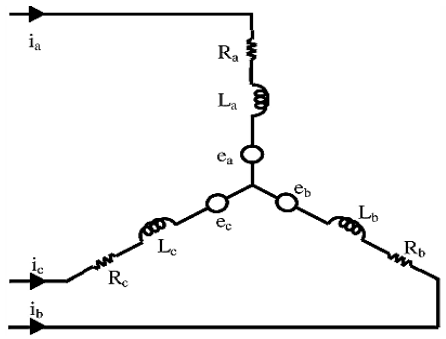

Figure 1. BLDC motor equivalent circuit

While the commutation in ordinary DC motors is carried out manually using a mechanical commutator and brushes, it is carried out electronically in BLDC motors utilizing hall-effect sensors and an electric inverter. BLDC motor's windings are located on either the rotor has been made of permanent magnets mounted on a steel core or stator and the rotor is built entirely of materials that are permanent magnets. Figure 1 depicts how the BLDC motor drive is set up. Hall-effect sensors use commutating signals to identify the position of the rotor. Similar to permanent magnet brushes are not required if the armature windings of the BLDC motor are replaced. Figure 2 illustrates the 3-phase BLDC motor's trapezoidal back-EMFs and square-wave phase currents with a 120° conduction mode [17].

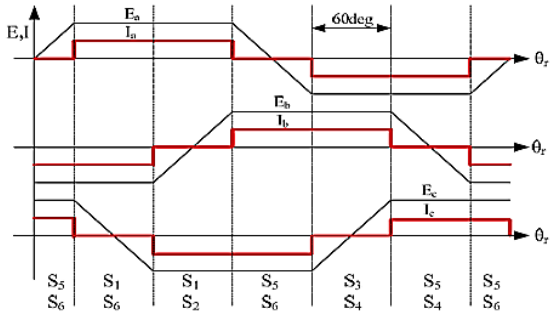

Figure 2. Back-emf and current waveforms

General voltage eq. of BLDC motor may be expressed below [18]:

$$\begin{bmatrix} V_a \\ V_b \\ V_c \end{bmatrix} = \begin{bmatrix} R_s & 0 & 0 \\ 0 & R_s & 0 \\ 0 & 0 & R_s \end{bmatrix} \begin{bmatrix} i_a \\ i_b \\ i_c \end{bmatrix} + \begin{bmatrix} La & Lab & Lac \\ Lba & Lb & Lbc \\ Lca & Lcb & Lc \end{bmatrix} \frac{d}{dt} \begin{bmatrix} i_a \\ i_b \\ i_c \end{bmatrix} + \begin{bmatrix} e_a \\ e_b \\ e_c \end{bmatrix} \quad (1)$$

La=Lb=Lc=Ls

L =L =L =M=0

$\boldsymbol{V_a}, \boldsymbol{V_b}, \boldsymbol{V_c}$ represent motor three-phase voltage values, $\boldsymbol{i_a}$, $\boldsymbol{i_b}, \boldsymbol{i_c}$ are motor three-phase currents, $\boldsymbol{e_a}$, $\boldsymbol{e_b}, \boldsymbol{e_c}$ represent motor three-phase back-emf wave-forms, *Rs* is motor phase resistance, La=Lb=Lc=L represents self-inductance of Electro-magnetic torque may be illustrated as:

$$T_e = (e_a i_a + e_b i_b + e_c i_c)/\omega_r \quad (2)$$

The represents electro-magnetic torque and represents mechanical speed. The BLDC motor motion equation can be expressed as:

$$J_s \dot{\omega}_r + B_s \dot{\omega}_r = T_e - T_L \quad (3)$$

T_L epresents load on motor shaft, J_s represents inertia moment of drive plus load and *Bs* represents constant of friction. Electrical frequency in terms of mechanical speed for motor rotor with *p* numbers of poles would be represented as [17]:

$$\theta_e = \frac{P}{2}\theta_m \quad (4)$$

where, ω_r: Angular speed of rotor, θ_m: Mechanical angle of rotor and θ_e: Electrical angle of rotor.

$$\omega_r = d\theta_m/dt \quad (5)$$

State space form of such system is shown in reference [17]:

$$\dot{X} = AX + BU \tag{6}$$

where,

$$X^T = [\, i_a \; i_b \;\; i_c \;\; \omega_r \;\; \theta_m \,], \tag{7}$$

$$U^T = [\, V_a \; V_b \;\; V_c \;\; T_L] \tag{8}$$

$$\dot{X} = \begin{bmatrix} A_{11} & 0 & 0 & A_{14} & 0 \\ 0 & A_{22} & 0 & A_{24} & 0 \\ 0 & 0 & A_{33} & A_{34} & 0 \\ A_{41} & A_{42} & A_{43} & A_{44} & 0 \\ 0 & 0 & 0 & 1 & 0 \end{bmatrix} X + \begin{bmatrix} B_{11} & 0 & 0 & 0 \\ 0 & B_{22} & 0 & 0 \\ 0 & 0 & B_{33} & 0 \\ 0 & 0 & 0 & B_{44} \\ 0 & 0 & 0 & 0 \end{bmatrix} \begin{bmatrix} V_a \\ V_b \\ V_c \\ T_L \end{bmatrix} \tag{9}$$

$$A_{11} = A_{22} = A_{33} = -\frac{R_S}{L}\; A_{14} = -\frac{\lambda m}{L} F(\theta_e)\; A_{24} = -\frac{\lambda m}{L} F\left(\theta_e - \frac{2\pi}{3}\right) A_{34} = -\frac{\lambda m}{L} F\left(\theta_e + \frac{2\pi}{3}\right) A_{41} = \frac{\lambda m}{J} F(\theta_e)\; A_{42} = \frac{\lambda m}{J} F\left(\theta_e - \frac{2\pi}{3}\right) A_{43} = \frac{\lambda m}{J} F\left(\theta_e - \frac{2\pi}{3}\right) A_{44} = -\frac{B}{J}\; B_{11} = B_{22} = B_{33} = \frac{1}{L}\; B_{44} = \frac{1}{J}$$

$$y = \begin{pmatrix} 1 & 0 & 00 & 0 \\ 0 & 1 & 00 & 0 \\ 0 & 0 & 10 & 0 \\ 0 & 0 & 01 & 0 \\ 0 & 0 & 00 & 1 \end{pmatrix} \begin{bmatrix} i_a \\ i_b \\ c \\ \omega_r \\ \theta_m \end{bmatrix} \tag{10}$$

The non-linear function $F(\theta_e)$ may be described as:

$$F(\theta e) = \begin{pmatrix} \frac{3}{\pi}(\theta_e), & 0 < \theta_e < \frac{3}{\pi} \\ 1, & \frac{3}{\pi} < \theta_e < \frac{2\pi}{3} \\ \mathbf{1} + \frac{\mathbf{3}}{\boldsymbol{\pi}}\left(\boldsymbol{\theta_e} - \frac{\mathbf{2\pi}}{\mathbf{3}}\right), & \frac{\mathbf{2\pi}}{\mathbf{3}} < \boldsymbol{\theta e} < \boldsymbol{\pi} \\ -\frac{3}{\pi}\left(\theta_e - \frac{2\pi}{3}\right), & \pi < \theta_e < \frac{4\pi}{3} \\ -1, & \frac{4\pi}{3} < \theta_e < \frac{5\pi}{3} \\ -1 - \frac{3}{\pi}\left(\theta_e - \frac{2\pi}{3}\right), & \frac{5\pi}{3} < \theta_e < 2 \end{pmatrix} \tag{11}$$

Figure 3 Schematic of the employed closed loop control system of BLDC motor with estimation in the feedback loop. Estimation inputs are operating voltages V_a, V_b and V_c or the motor's phases A, B and C, while outputs are estimated values of angular speed $\hat{\omega}_r$ and rotor's angular position $\hat{\theta}_m$.

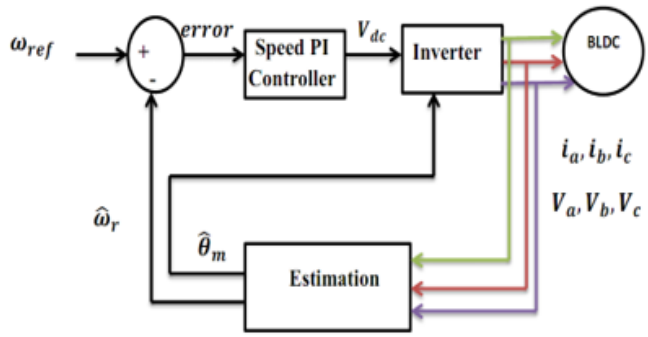

Figure 3. Diagram of estimation

3. THE PROPOSED APPROACH

In this section, the Particle Filter (PF) method, and its two Extended Kalman Filter (EKF) proposed in the present work have been explained in detail.

3.1 Extended Kalman Filter (EKF)

Kalman filter was designed specifically for linear systems. However, many real-world systems, like BLDC motors, are non-linear. If the nonlinearities are minimal, they can be ignored. Despite their importance, they are frequently overlooked. Non-linearity is a phenomenon that occurs when there is a change that cannot be overlooked and must be compensated in some way Before a Kalman filter can be applied to the system, it must first pass one of these tests. Non-linear equations can be linearized in some ways [19].

The Taylor series can be used to get around a given working point. The Taylor series is used to solve nonlinearities in a system. Using these equations, a variant of the Kalman filter is known as Extended Kalman Filter. This observer has the ability to almost every non-linear system can be handled at a low cost. At each time sample, the Taylor series is calculated. Although Extended Kalman Filter can't be proven to be optimal, this doesn't imply that it is a terrible solution. Because BLDCM is an engine without a coil brush then requires BLDC position sensor to rotate the rotor this is a weakness of BLDC. Suggest an algorithm without sensors like the Extended Kalman Filter (EKF) to cover this weakness. In addition, BLDC is also a non-linear system. So using the EKF algorithm, which can be linearized using Jacobian matrix, we can get the stability of the system. The non-linear variant of Kalman filter, on the other hand, usually performs admirably. The Extended Kalman Filter is required to continually predict speed and position rotor of BLDC motor utilizing recorded voltages and currents. The motor current is estimated in each time step [20]. Generally, EKF's estimating system is divided into two stages: the step of prediction and the step of correction The predicted state variable value and predicted state variable value are calculated in the first stage. The expected state covariance Matrix is denoted by $\frac{Pk}{k} - 1$, can be obtained, and a correction term is added to the anticipated value in the second stage, the corrective step $\tilde{X}k/k$ [18-24].

The estimation procedures for the EKF can be listed as follow [21, 22]:

1-Prediction of State:

$$\tilde{X}k/k - 1 = f\left(\tilde{X}k - \frac{1}{k} - 1, Uk - 1\right) \tag{12}$$

2-Error Covariance Matrix Estimation:

$$Pk/k - 1 = \emptyset k - 1Pk - 1/k - 1\emptyset k - 1^T + Qk - 1 \tag{13}$$

3-Computation of Kalman Filter Gain:

$$K_K = Pk/k - 1H^T(HPk/k - 1H^T + R_K)^{-1} \tag{14}$$

4-State Estimation

$$\begin{aligned} \tilde{y}_k &= y_k - H(\tilde{X}k/k - 1) \\ \tilde{X}k/k &= \tilde{X}k/k - 1 + K_K\, \tilde{y}_k \end{aligned} \tag{15}$$

5-Update of Error Covariance Matrix:

$$Pk/k = (1 - K_K\ H_K)Pk/k - 1 \tag{16}$$

3.2 Particle Filter (PF)

Utilizing all of the available information, which include the measurement data, in order to create posterior probability density function (pdf) is one option for state estimate based upon Bayesian filtering method. It is possible to determine optimum state estimation and its precision from this pdf because it comprises all statistical data. A posterior pdf is produced by applying Bayes' rule [22]:

$$\boldsymbol{p(X_k|Y_{1:k})} = \frac{\boldsymbol{p(Y_k|X_k)p(X_k|Y_{1:k})}}{\boldsymbol{p(X_k|Y_{1:k})}} \tag{17}$$

In (17):

$$\begin{aligned} &\boldsymbol{p(X_k|Y_{1:k-1})} \\ &= \int \boldsymbol{p(X_k|X_{1:k-1})\, p(X_{k-1}|Y_{1:k-1})dX_{1:k-1}} \\ &\boldsymbol{p(Y_k|Y_{1:k-1})} = \int \boldsymbol{p(Y_k|X_k)\, p(X_k|Y_{1:k-1})dX_k} \end{aligned} \tag{18}$$

Except a few cases (such as the linear Gaussian model), there are no analytical solutions to those equations. For other models, (18) must be approximately evaluated. Particle Filter has been represented for the approximation of the posterior pdf through the utilization of a group of the random weighted particles$\{(X_k^n, W_k^n), n = 1{:}\,N\}$ [21],

$$\boldsymbol{p(X_k|Y_{1:k-1})} \approx \sum_{m=1}^{N} W_k^m\, \delta(X_k - X_k^m) \tag{19}$$

where, X_k^m represents state value of the mth particle, W_k^m its weight, $\delta(.)$ represents Dirac delta function, and N represents number of particles. In fact, particle weight shows the potential of a particle being represented by Eq. (19)

$$w_k^{(i)} \propto w_{k-1}^{(i)} \frac{\boldsymbol{p(Y_k|X_k)p(X_k|Y_{1:k})}}{\boldsymbol{q(X_k|Y_k)}} \tag{20}$$

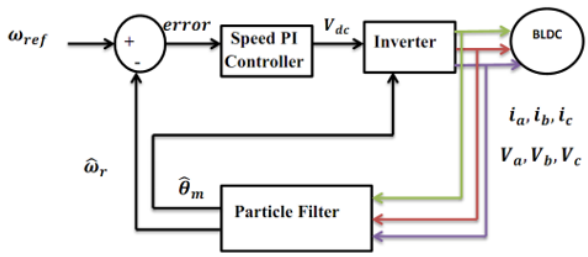

Figure 4. The structure of the suggested sensorless speed control drive

The use of the Particle Filter to estimate state is a recursive technique. Most particles will have modest weights after numerous repetitions. As a result, a significant amount of computing time is spent updating particles that play a minor role in estimating the pdf. Degeneracy is the term for this situation, which is a prevalent PF issue. Degradation is the term for this situation, and it is a prevalent problem in PF. This situation often affects the implementation of the Particle Filter. To avoid this situation use methods including resampling to maintain the performance of the PF. One of the most well-known strategies for preventing degeneracy is the use of Re-sampling Small-weight particles are duplicated with large-weight particles throughout the process of re-sampling.

$$\dot{X} = f(X)X + Bu \tag{21}$$

Figure 4 shows that through the use of measuring currents and voltages, velocity and momentum can be measured without a sensor by relying on the Particle Filter.

Consider the following nonlinear system using state equations:

$$\dot{X} = f\big(X(t)\big)X(t) + Bu(t) + \sigma(t) \tag{22}$$

$$y(t) = h\big(X(t)\big) + v(t) \tag{23}$$

σ(t) & v(t) represent zero-means white Gaussian noises with Q(t) and R(t) covariance, respectively. Eq. (22) and Eq. (23) are in continuous time domain, however, PF algorithm has been implemented in the discrete domain. Those equations can be represented in the following forms:

$$X_{k+1} = (I + f(X_k)\Delta t)X_k + B\Delta t u_k + w_k \tag{24}$$

$$y_k = h(X_k) + v_k \tag{25}$$

The identity matrix is I, and the sampling time is t. Process and measurement noises pdf are expected to be known in these equations.

N initial particles ($X_{0.i}^{+}$(i= 1.....N)) are created randomly in the first iteration, based upon initially presumed p(X_0). The choice of parameter N in a Particle Filter has a significant impact on estimation accuracy and computational load. Parameter N is a set of particles that can determine the appropriate value of parameter N when obtaining better stability of the system.

Initial particles have been propagated in system discrete Eq. (24) to get prior particles $X_{k.i}^{-}$. In the next phase, each preceding particle must be given a relative weight based on the measurement results. This is accomplished by assessing the p($y_k|x_k$) and determining the particle likelihood as follows [22]:

$$q_i = \mathrm{p}(y_k|x_{k.i} \sim 1/(2\pi)^m/2\ |R|^{\frac{1}{2}} \exp\,(-[y - h(X_k)]^T\, R^{-1}[y - h(X_k)]\,/\,2) \tag{26}$$

where, m refers to output matrix dimension and y refers to the measured data. The weight of every one of the particles is directly proportionate to its probability, according to Eq. (19) and (25). After that, resampling based on normalized likelihood is used to choose large-weighted particles and generate posterior particles $X_{k.i}^{+}$. The posterior p($X_k|y_{k.i}$) is now computed. Finally, the average of approximated p($X_k|y_{k.i}$) is calculated to produce the state estimation. It's worth noting that these posterior particles are transmitted to form previous particles in the next iteration.

The ~ symbol in the above equation means that the probability is not really given by the expression on the right side, but the probability is directly proportional to the right side. So if this equation is used for all the particles $X_{k.i}^{-}$. (i = 1... , N), now we normalize the relative likelihoods obtained in

Eq. (26) as follows.

$$qi = \frac{qi}{\sum_{j=1}^{N} qj} \tag{27}$$

This ensures that the sum of all the likelihoods is equal to one. Next we resample the particles from the computed likelihoods. That is, we compute a brand new set of particles $X_{k.i}^{+}$ that are randomly generated on the basis of the relative likelihoods qi [21].

Figure 5 shows the steps for implementing a Particle Filter.

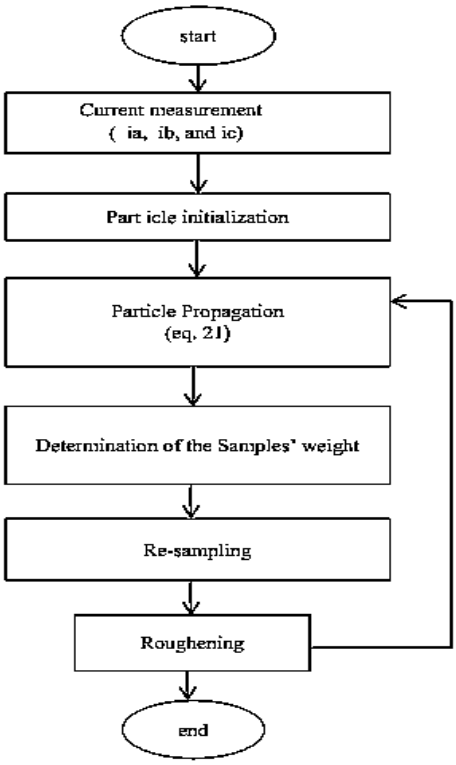

Figure 5. The flowchart of the proposed PF algorithm

4. SIMULATION AND IMPLEMENTATION

The simulation model of BLDC Motor and results was implementation based on MATLAB programming. The table 1 show simulation parameter of the BLDC motor. The Simulink block of our model has the EKF and PF algorithm when PF blocks input. The PF block's inputs are the measured currents and line voltages. Following a formatted explanation of the PF algorithm's operation in the third part, estimated speed and position were employed at each time step. Feedback from the driving system. Any measurement data in a real-time system has noise and error.

Table 1. Parameters of BLDC motor

Rated voltage	80V
Rated speed	1500rpm
Rotor Inertia - J_s [kg-m^2]	5.5e-3
Resistance – R_s	1.43ohm
Inductance – L	9.4e-3H
Friction Coefficient	2e-3
Torque constant	3N.m
Rotor Flux	0.2158wb
Number of pole pairs (P)	4

Based upon the mathematical Eq. (1) in order to obtain a prediction ω, data that are required includere ia, ib, ic, va, vb, vc, TL, and ωr at previous time. The process of the prediction is performed with the use of EKF algorithm and PF algorithm. In such case, ia, ib, ic, va, vb, and vc is created by taking direct measurements. Two treatments have been done in order to verify performance of velocity and modification load to justify the estimated performance of our method. In this example, reference speed is modified from 750 to 1500 r.p.m at time t = 0.6 s. after that, load torque TL = 3 is added to this motor at time t = 2 s. Figure 6a shows the Simulink model of BLDC motor with EKF

Figure 6b illustrates connection of Simulink model to the EKF. By relying on the measurement of currents and voltages, we will obtain the measurement of velocity and position.

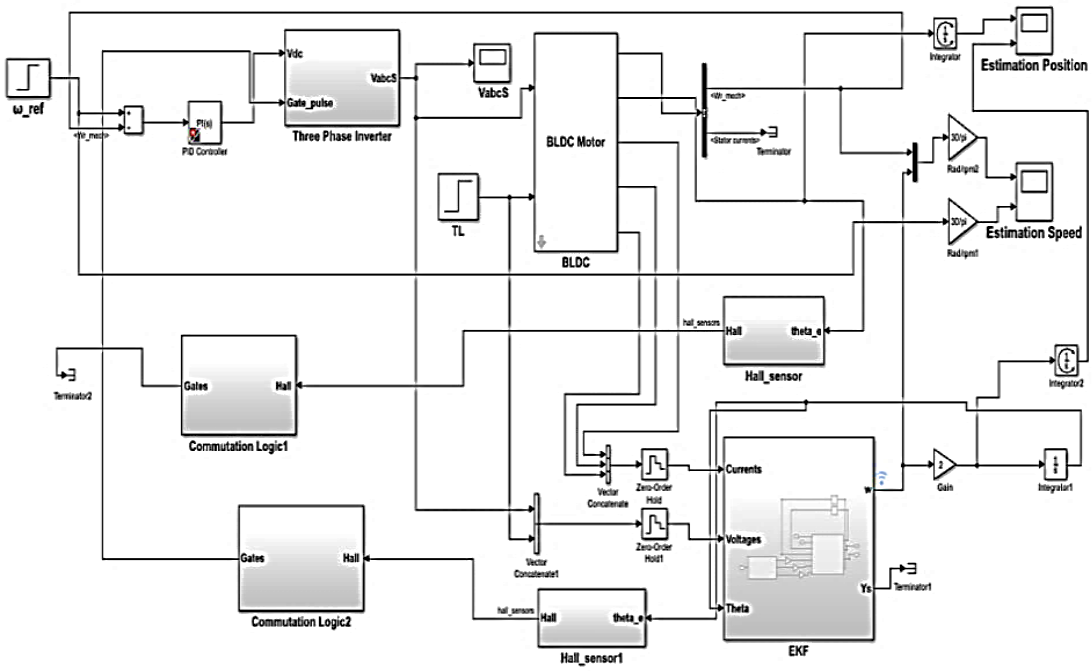

(a) Simulink model of BLDC motor with EKF

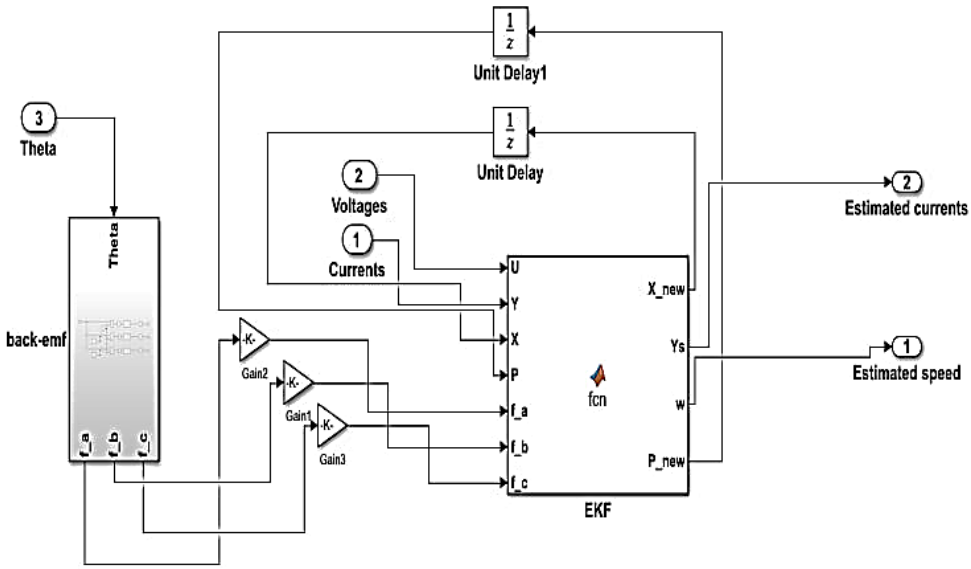

(b) Simulink model to the EKF

Figure 6. (a) Simulink model of BLDC motor with EKF; (b) Simulink model to the EKF

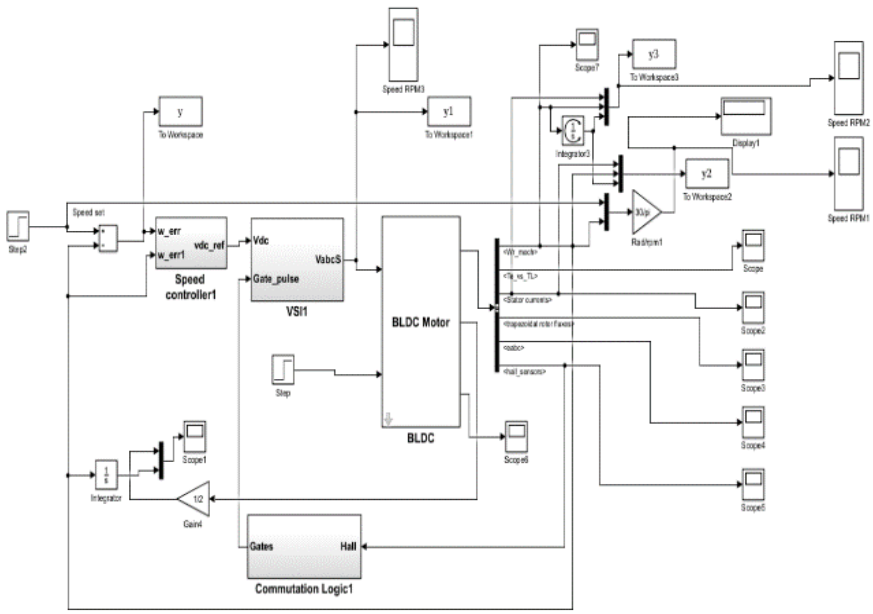

Figure 7. Simulink model of real system BLDC motor

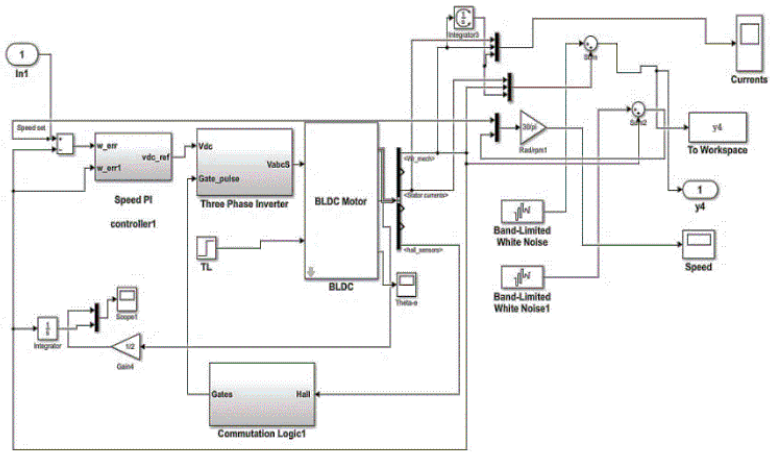

Figure 8. Simulink model of BLDC motor with PF

Figure 7 shows Simulink model of the real system forBLDC Motor, while Figure 8 shows Simulink model of BLDC Motor with Estimation. The comparison between the two systems is done by relying on a Particle Filter (PF).

Figure 9 shows speed of BLDC Motor with EKF When loading within t=2s, the amount of TL = 3 N.m becomes 1490rpm when loaded with estimation, and the speed with optimum is 1470rpm. After that, when the load is lifted, both speeds stabilize with the reference speed of 1500rpm, and as we note the error speed at EKF is about 1% and Figure 10 shows the position at EKF. From the figure, we notice the error position of 0.314%. While Figure 11 shows the speed of BLDC motor with PF, the speed at load is 1495, and as we note error speed = 0.01% and error position = 0.112%. Figure 12 shows the rotor position of the BLDC Motor while Figure 13 shows current with estimation and Figure 14 shows current without estimation.

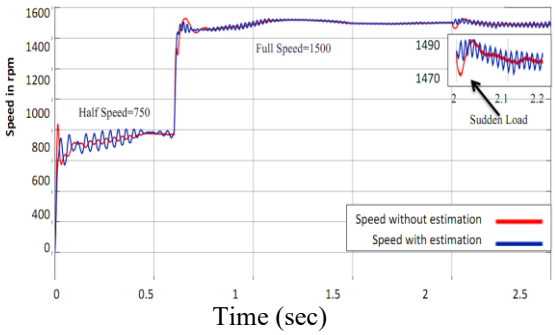

Figure 9. Shows the speed of BLDC Motor with EKF under TL=3N.m

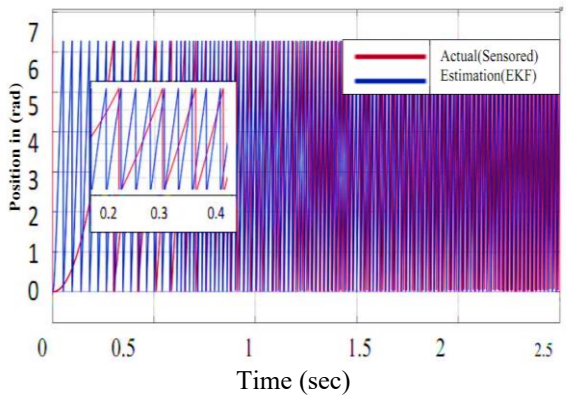

Figure 10. shows the rotor position of BLDC Motor PF

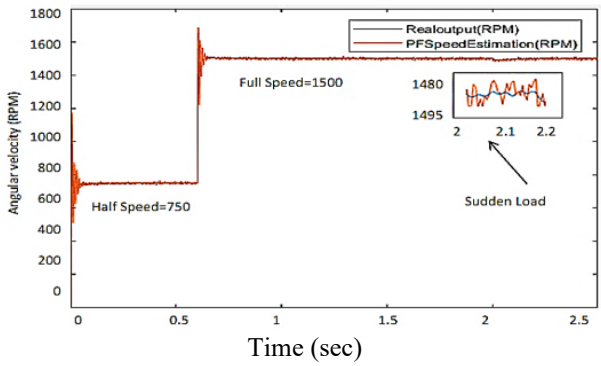

Figure 11. Shows the speed of BLDC Motor with PF under TL=3N.m

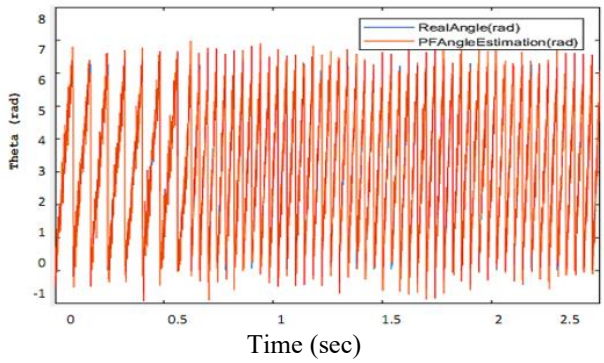

Figure 12. The rotor position of BLDC Motor with PF

This work has been compared with previous studies and Table 2 illustrates this.

Table 2. Showing the comparison between previous studies and current work

Senserless	Error speed	Error position
EKF	1%	0.314%
Unkf [10]	3%	2%
PF	0.01%	0.112%

The reason that confirmed that the PF is the best through the results gave a better result than the rest of the filters through the error speed ratio were 0.01% and the position ratio was equal to 0.112. It also gave the best stability of the system at 1s. As shown in the table2, the improvement rate at PF is better than the ratio of UKF, and EKF found the percentage of improvement is of 3% and 2% speed and position respectively.

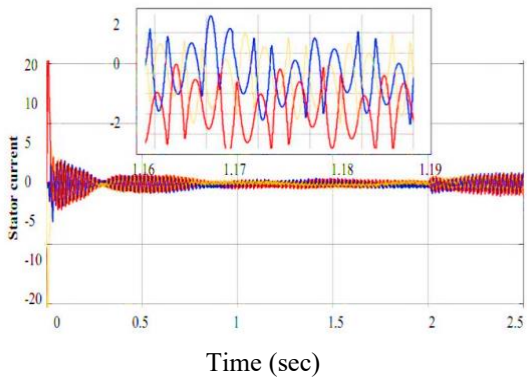

Figure 13. Three-phase stator current with the estimation

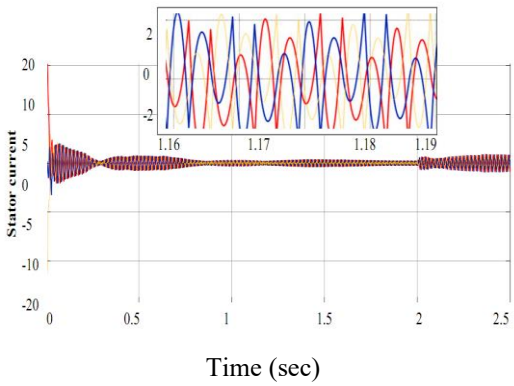

Figure 14. Three-phase stator current without estimation

5. CONCLUSIONS

In the presented paper, for the purpose of operating non-sensor BLDC motor, a new classification system had been developed for rotor speed and rotor position speed with the use of an EKF and a particulate filter (PF). An accurate estimation performance may be obtained from results of simulation and efficiency of the suggested designed model can be demonstrated. The two proposed algorithms can maintain the motor speed with a speed error of 1% at EKF, 0.01% at PF, and a position error of about 0.314% at EKF, while at PF about 0.112%. Through this, it was found that PF gave better results compared to EKF. In addition, the precision sensorless BLDC motor may be controlled as well according to the algorithm that has been designed for EKF and PF. It was also proven by comparing the previous studies and this work and found the percentage of improvement is of 3% and 2% speed and position respectively.

REFERENCES

[1] Abood, L.H., Haitham, R. (2022). Design an optimal fractional order PI controller for congestion avoidance in internet routers. Mathematical Modelling of Engineering Problems, 9(5): 1321-1326. https://doi.org/10.18280/mmep.090521

[2] Yasien, F.R., Mahmood, R.A. (2018). Design new control system for brushless DC motor using SVPWM. International Journal of Applied Engineering.

[3] Ezzaldean, M.M., Kadhem, Q.S. (2019). Design of control system for 4-switch bldc motor based on sliding-mode and hysteresis controllers. Iraqi Journal of Computers, Communications, Control and Systems Engineering, 19(1): 42-51. https://doi.org/10.33103/uot.ijccce.19.1.6

[4] Hameed, H.S. (2018). Brushless DC motor controller design using MATLAB applications. In 2018 1st International Scientific Conference of Engineering Sciences-3rd Scientific Conference of Engineering Science (ISCES), pp. 44-49. https://doi.org/10.1109/ISCES.2018.8340526

[5] Boussekra, F., Makouf, A. (2020). Sensorless speed control of IPMSM using sliding mode observer based on active flux concept. Modelling, Measurement and Control A, 93(1-4): 1-9. https://doi.org/10.18280/mmc_a.931-401

[6] Sivakami, R., Sugumar, G. (2019). Speed control of sensorless brushless DC motor by computing back emf from line voltage difference. International Journal of Electrical Engineering & Technology, 10(5): 31-38. https://ssrn.com/abstract=3554218.

[7] Akkar, H.A., Salman, S.A. (2020). Improvement parameters for design brushless DC motor by moth flame optimization. In IOP Conference Series: Materials Science and Engineering, 745(1): 012019-012019. https://doi.org/10.1088/1757-899X/745/1/012019

[8] Boiko, Y., Lin, C., Kiringa, I., Yeap, T. (2021). Performance of BLDC motor under Kalman filter sensorless drive. International Journal of Electrical and Information Engineering, 15(7): 282-288.

[9] Aishwarya, V., Jayanand, B. (2016). Estimation and control of sensorless brushless dc motor drive using extended kalman filter. In 2016 International Conference on Circuit, Power and Computing Technologies (ICCPCT), 1-7. https://doi.org/10.1109/ICCPCT.2016.7530343

[10] Rif'an, M., Yusivar, F., Kusumoputro, B. (2018). Design of extended kalman filter speed estimator and single neuron-fuzzy speed controller for sensorless brushless DC motor. Journal of Telecommunication, Electronic and Computer Engineering (JTEC), 10(1-5): 157-161.

[11] Ellahi, N. (2021). Extended kalman filter based brushless dc motor for rotor position and speed control.

[12] Vinida, K., Chacko, M. (2021). Implementation of speed control of sensorless brushless DC motor drive using H-infinity controller with optimized weight filters. International Journal of Power Electronics and Drive Systems, 12(3): 1379-1379. https://doi.org/10.11591/ijpeds.v12.i3.pp1379-1389

[13] Chojowski, M. (2018). Simulation analysis of extended Kalman filter applied for estimating position and speed of a brushless DC motor. Power Electronics and Drives, 3(1): 145-155. https://doi.org/10.2478/pead-2018-0008

[14] Rif'an, M., Yusivar, F., Kusumoputro, B. (2019). Sensorless-BLDC motor speed control with ensemble Kalman filter and neural network. Journal of Mechatronics, Electrical Power, and Vehicular Technology, 10(1): 1-6. https://doi.org/10.14203/j.mev.2019.v10.1-6

[15] Lv, H., Wei, G., Ding, Z., Ding, X. (2015). Sensorless control for the brushless DC motor: An unscented Kalman filter algorithm. Systems Science & Control Engineering, 3(1): 8-13. https://doi.org/10.1080/21642583.2014.982769

[16] Rif'an, M., Yusivar, F., Kusumoputro, B. (2018). Design of extended kalman filter speed estimator and single neuron-fuzzy speed controller for sensorless brushless DC motor. Journal of Telecommunication, Electronic and Computer Engineering (JTEC), 10(1-5): 157-161.

[17] Ali, Q.M., Ezzaldean, M.M. (2020). Direct current deadbeat predictive controller for bldc motor using single dc-link current sensor. Engineering and Technology Journal, 38(8): 1187-1199. https://doi.org/10.30684/etj.v38i8A.471

[18] Abedulabbas, G.W., Yaseen, F.R. (2022). Design a PI controller based on PSO and GWO for a brushless DC motor. Journal Européen des Systèmes Automatisés, 55(3): 331-338. https://doi.org/10.18280/jesa.550305

[19] Alawsi, A.A.A., Jasim, B.H., Raafat, S.M. (2019). Nonlinear estimation of quadcopter states using unscented Kalman filter. Periodicals of Engineering and Natural Sciences, 7(4): 1626-1637. http://dx.doi.org/10.21533/pen.v7i4.878

[20] Alpago, D., Dörfler, F., Lygeros, J. (2020). An extended Kalman filter for data-enabled predictive control. IEEE Control Systems Letters, 4(4): 994-999. https://doi.org/10.1109/LCSYS.2020.2998296

[21] Rif'an, M., Yusivar, F., Wahab, W., Kusumoputro, B. (2015). A comparison of ensemble Kalman filter and extended Kalman filter as the estimation system in sensorless BLDC motor. ARPN Journal of Engineering and Applied Sciences, 10(17): 7386-7393.

[22] Yasien, F.R., Khalid, H.W. (2017). Sensorless speed estimation of permanent magnet synchronous motor using extended kalman filter. Iraqi Journal of Computers, Communications, Control & 21 Systems Engineering (IJCCCE), 18(1): 64-81.

https://doi.org/10.33103/uot.ijccce.18.1.7
[23] Chulaee, Y., Zarchi, H.A., Sabzevari, S.I.H. (2019). State estimation for sensorless control of BLDC machine with particle filter algorithm. In 2019 10th International Power Electronics, Drive Systems and Technologies Conference (PEDSTC), 172-177. https://doi.org/10.1109/PEDSTC.2019.8697632
[24] Sabzevari, S.I.H., Chulaee, Y., Abdi, S. (2020). Analysis and modification of a particle filter algorithm for sensorless control of BLDC machine. In 2020 International Conference on Electrical Machines (ICEM), 1: 1067-1073. https://doi.org/10.1109/PEDSTC.2019.8697632